

RSC Advances



This is an *Accepted Manuscript*, which has been through the Royal Society of Chemistry peer review process and has been accepted for publication.

Accepted Manuscripts are published online shortly after acceptance, before technical editing, formatting and proof reading. Using this free service, authors can make their results available to the community, in citable form, before we publish the edited article. This *Accepted Manuscript* will be replaced by the edited, formatted and paginated article as soon as this is available.

You can find more information about *Accepted Manuscripts* in the [Information for Authors](#).

Please note that technical editing may introduce minor changes to the text and/or graphics, which may alter content. The journal's standard [Terms & Conditions](#) and the [Ethical guidelines](#) still apply. In no event shall the Royal Society of Chemistry be held responsible for any errors or omissions in this *Accepted Manuscript* or any consequences arising from the use of any information it contains.



Journal Name

ARTICLE

Adjusting phase transition of titania-based nanotubes via hydrothermal and post treatment

Haiqiang Lu^{*a}, Ying Wang^a, Yuanyang Wang^a, Wensheng Liang^a and Jianfeng Yao^{*b}

Received 00th January 20xx,
Accepted 00th January 20xx

DOI: 10.1039/x0xx00000x

www.rsc.org/

Titania-based nanotubes are prepared via hydrothermal and post treatment of titania with different anatase/rutile ratios. Commercial TiO₂ P25 with anatase/rutile ratio of 80/20 changes to sodium titanate, hydrogen titanate and anatase after hydrothermal treated at 130 °C over 2 h, ion exchange by washing with water and calcination at 400 °C for 5 h. The final tubular structure has a lot of defects owing to a great quantity of dehydration. Pure rutile is more stable than P25. Lamellars exfoliate from (110) facet of rutile at 130 °C hydrothermal treatment to roll up into nanotubes. Only small amount of rutile transfers to amorphous sodium titanate within 24 h, and it recrystallizes on the surface of nanotubes and results in a perfect tubular structure with a small amount of dehydration. The dissolution-recrystallization mechanism plays an important role in the composition and crystal structure of titania-based nanotubes.

1. Introduction

High-quality one-dimensional (1D) titania-based nanostructures have been attracting attentions during the past decades. Taking advantage of their unique physical-chemical properties, such as high aspect ratio, high photostability and non-hazard, there were excellent performances as sensors, photovoltaic cells and (photo)catalysts.¹ The titania-based nanostructures can be cheaply obtained by treating TiO₂ nanoparticles in a concentrated NaOH solution under mild conditions benefiting from Kasuga's pioneering work,^{2,3} which then opens a continuous and interesting research direction.

The preparation parameters, including the hydrothermal temperature and duration,⁴⁻⁶ alkali concentration,⁷ crystalline structure and particle size of the starting precursor,⁸⁻¹¹ washing procedure and calcination temperature,^{12,13} would affect the morphology of 1D titania-based nanostructures. The formation mechanisms have been widely studied.^{9,14-23} But there are a lot of contradictory results, and it is very hard for researchers to fully understand the process. The 1D nanostructures have molecular compositions of Na_xH_yTi_mO_n, and H_xTi_yO_z after sodium exchange, which can be translated into anatase TiO₂ after calcination at an optimal temperature. However, the formation mechanism of 1D nanostructures still remains disputed. Although the hydrothermal method is relatively simple, it is a complex process that includes many

complicated changes. To date, there are various formation mechanisms of 1D nanostructures, including rolling-up mechanism, oriented crystal growth (OCG) process, dissolution-recrystallization mechanism, oriented attachment (OA) and Ostwald ripening (OR) mechanism. One or some of the mechanisms might be employed to explain the formation process of 1D structure.²⁴⁻²⁶ Previously we have presented an overall picture of the transformation process that can record all the nanostructures (nanoparticles, nanosheets, nanotubes, and nanowires) during the alkali hydrothermal process by subtly controlled termination of reaction and capture of intermediates, mainly by shortening the sampling intervals as far as possible. We captured the key intermediates and focused on their morphology, with the aim of obtaining a reasonable mechanism that can rationally clarify the formation of discrepant 1D nanostructures. Based on the solid evidence, we proposed that raw TiO₂ nanoparticles initially aggregate into large powders via oriented attachment mechanism, and then lamellar nanosheets exfoliate from the large particles and roll into short nanotubes. Afterwards, the short nanotubes transform into long ones through head-to-head attachment (oriented attachment) and Ostwald ripening. The long nanotubes further assemble into shoulder-to-shoulder bunches and continue to self-integrate into crystallized nanowires. Here, the oriented attachment mechanism plays a vital role throughout the hydrothermal process.²³ It is undoubtedly reasonable that the mechanism of the hydrothermal treatment was obtained via morphological characteristics of intermediates.

However, the composition and phase transition of the products greatly differ from one to another. In fact, the elimination of discrepancies might mainly depend on a lot of factors, such as the dissolution-recrystallization process. Based on the elaborated study of the form mechanism via the

^aSchool of Chemical and Biological Engineering, Taiyuan University of Science and Technology, Taiyuan 030024, China. E-mail: luhaqiang-1900@163.com

^bCollege of Chemical Engineering, Nanjing Forestry University, Nanjing 210037, China. E-mail: jfyao@njfu.edu.cn

Electronic Supplementary Information (ESI) available: [TG-DSC curves of titanate nanotubes; TEM images of hydrogen titanate nanotubes; XRD patterns (a) and Raman spectra (b) of hydrothermal products using P25-700-1; SEM image of the hydrothermal product using P25-800-8; XRD patterns of hydrothermal products using P25-800-8 for 2-10 days]. See DOI: 10.1039/x0xx00000x

morphological characteristics in hydrothermal process,²³ the phase transition of the products has been further understood. Moreover, high-quality pure one-dimensional titania nanostructures have more wide applications in various fields as compared to sodium titanate or hydrogen titanate. The main goal of the present work is to gain subtle and systematic control on the crystal structures of the 1D nanostructures by hydrothermal and post treatment, which can obtain nanotubes with different anatase/rutile ratios. Detailed characterizations of the prepared materials by means of XRD, Raman spectroscopy, UV-Visible, TEM, FT-IR and N₂ sorption isotherms were conducted to obtain the crystalline transformation of the 1D nanostructure by using different raw materials with various anatase/rutile ratios in order to achieve common knowledge. In view of these systematic results, the mechanism of the 1D nanostructures was discussed in details.

2. Experimental section

2.1. Preparation of various titania-based nanomaterials

Sodium titanate nanowires were synthesized at 150 °C in 10 M NaOH for 120 h by using 0.5 g of P25. The precipitates were collected and washed with deionized water until the pH was ~7. The nanowires will be sequentially immersed in 500 mL of deionized water for 1-5 days, where the Na⁺ ions are partly/totally replaced by H⁺ ions. The crystal transition of hydrogen titanate and sodium titanate was undertaken by calcination at 400 °C for 5 h.

Three types of TiO₂ with different anatase/rutile ratios were used as raw materials in the hydrothermal synthesis of nanotubes. TiO₂ crystal structure modulation was performed using a calcination method with commercial TiO₂ powder (P25, Degussa) as a starting material. The powder had an anatase/rutile ratio of about 80/20 and a specific surface area of about 50 m²/g. A typical calcination was carried out in a muffle furnace in air at 700 (for 1 h) and 800 °C (for 8 h), which resulted in the products with anatase/rutile ratios of about 40/60 and 0/100, respectively.

The crystal transition of titania-based nanotubes was carried out at 130 °C in 10 M NaOH for 0-24 h using the above three raw materials. The samples were immersed in deionized water for 5 days to eliminate the Na⁺ ions, and then they were sintered at 400 °C for 5 h.

2.2. Characterization

The phase structure of the TiO₂-based photocatalyst was examined by X-ray diffraction (XRD) using Rigaku MiniFlex II with Cu K α radiation ($\lambda=0.1542$ nm) at 40 kV. The UV-Vis absorption spectra were recorded on a Perkin-Elmer Lambda 750 UV/Vis/NIR Spectrometer. Raman measurements were performed on a Jobin-Yvon HR-800 Raman system, using the 514 nm line of an Ar laser as the excitation source. The morphology of the as-synthesized materials was characterized by field-emission scanning electron micrograph (FE-SEM). The SEM images were obtained using a Hitachi S-5500 scanning electron microscope. TEM images were taken on a JEM-2010 electron microscope operated at 200 kV. All samples were

prepared by suspension in ethanol and drop-cast onto a carbon-coated copper TEM grid. The specific surface areas were measured by the Brunauer-Emmett-Teller (BET) method employing nitrogen adsorption at 77 K after treating the samples at 100 °C and $\sim 10^{-4}$ Pa for 2 h using a Tristar-3000 apparatus.

3. Results and discussion

3.1 The phase transition of titania-based nanowires by post treatment

Analysis with XRD was made to observe the crystal structure and composition changes after hydrothermal and post treatment. Fig. 1a shows that the crystalline structure of commercial P25 TiO₂ (Degussa) possesses 80% anatase and 20% rutile. The alkali hydrothermal treatment is a kinetically controlled process, in which morphological transitions was strongly affected by the treating temperature and duration.^{15, 23} The successive appearance of nanosheets, nanotubes and nanowires are three unavoidable reaction steps. Increasing the hydrothermal temperature could only accelerate the nanotube/nanowire transformation process but could not affect the subsequence of the reaction.¹⁵ It is known that alkali metal titanates have a chemical formula of A₂Ti_nO_{2n+1} (A= alkali metal ion or proton, n= 2-9) with layered or tunnel-type crystal structures.²⁷ After a long hydrothermal treatment at 150 °C for 120 h, XRD peaks at $2\theta= 8.6^\circ$ and 10.6° , appear and they are ascribed to titanate crystals (sodium titanate Na₂Ti₃O₇ and hydrogen titanate H₂Ti₃O₇), which are due to the reaction of TiO₂ with the concentrated NaOH solution and the Na⁺ ions are partly replaced by H⁺ ions in 1 d washing (Fig. 1b). These results are almost fully in agreement with the discovery by Elsanousi et al.¹⁸, where commercial TiO₂ nanopowder (98%, Beijing chemicals Co.) with particle sizes of 50-400 nm as the starting material instead of P25 were hydrothermally treated at 180 °C for 72 h. This work further proved that increasing the temperature could accelerate the transition of composition and crystal structure of 1D nanostructures. It was also observed that a little H₂Ti₃O₇ appeared after washing with deionized water only. More hydrogen titanate was observed after keeping washing with deionized water for 3 d (Fig. 1c). It can be proved that the peak at $2\theta = 8.6^\circ$ disappeared after sintering at 400 °C for 5 h (Fig. 1d). Therefore, the hydrogen titanate to anatase phase transition could be initiated by dehydration. Fig. 1e clearly shows that all of the sodium titanate is transformed into hydrogen titanate by washed with deionized water only (5 d), and the hydrogen titanate is completely transformed into anatase titania with a high crystallinity after sintering at 400 °C for 5 h (Fig. 1f). Obviously, all the XRD characteristic peaks at $2\theta=25.1^\circ, 37.9^\circ, 48.2^\circ, 53.9^\circ, 55.3^\circ$ and 62.8° are assigned to (101), (004), (200), (105), (211) and (204) of the anatase TiO₂, respectively. The results show clearly that either sodium titanate nanowires or nanotubes can be transformed into hydrogen titanate via ion exchange, and then anatase phase by calcination at 400 °C for 5 h.

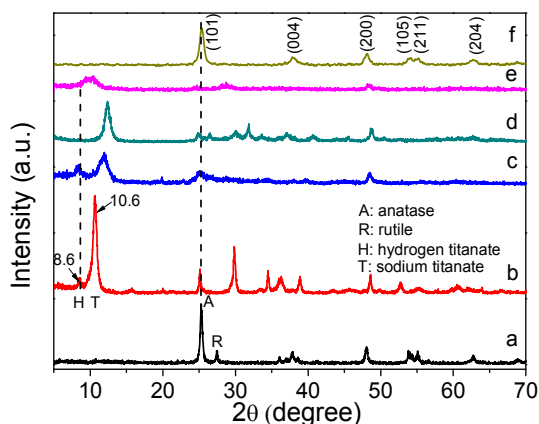
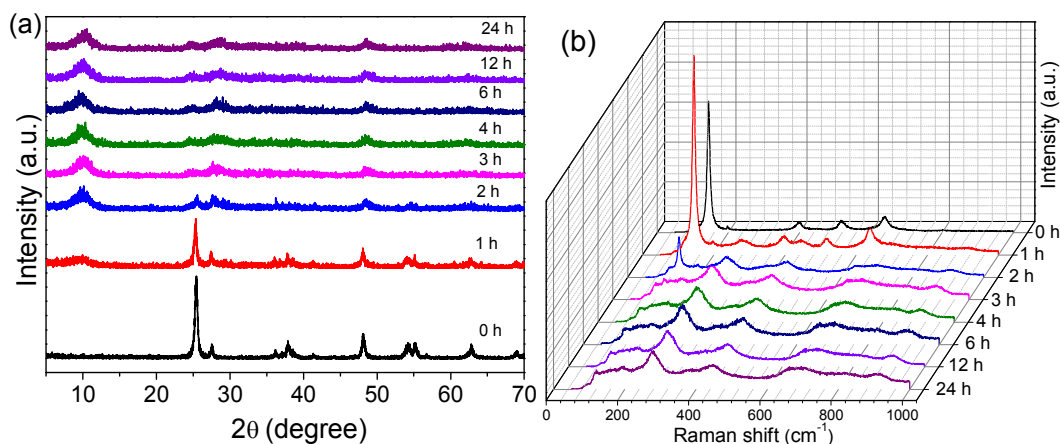


Fig. 1. XRD patterns of commercial P25 (a), the corresponding hydrothermal products synthesized at 150 °C for 120 h and washed for 1 (b), 3 (c), 5 d (e), and the sintered products (d) and (f) at 400 °C for 5 h by (c) and (e), respectively.

3.2 Phase transition of titania-based nanotubes using various types of TiO₂ as materials

Many titania resources were used as raw materials in the hydrothermal treatment to investigate the nanotube formation. Contradictory results are frequently obtained, where the formation mechanism and the relationship between treatment conditions and structure is not well established¹. In order to eliminate the parameter change effects as far as possible, all of the products by hydrothermal treatment were only washed with deionized water. The typical XRD patterns (Fig. 2a) indicate that P25 (anatase/rutile: 80/20) is turned into

sodium titanate and then hydrogen titanate in hydrothermal process. Little trace of anatase and rutile TiO₂ was detected. However, the nanotubes have quite high thermal stability, which can retain their tubular structure integrity up to 400 °C for 5 h after dehydration. At calcination temperatures above 400 °C, the nanotubes undergo a transformation to pure titania nanorods (Fig. S1 and S2). These results are almost fully in agreement with the discovery by Vijayan et al.¹². Fig. 2b shows that Raman spectra of the products have characteristic bands of H₂Ti₂O₅·H₂O phase (121, 193, 275, 445, 695, 910 cm⁻¹), which match well with the XRD results. Anatase phase is obviously unstable in a high concentrated alkali solution at 130 °C and it is almost transformed into sodium titanate in 2 h. However, pure rutile phase P25-800-8 is more stable in the process (Fig. 2c, d; P25-700-1 anatase/rutile: 40/60 in Fig. S3) and the morphology is changed from nanoparticles into nanotubes (Fig. S4). Little trace of alkali metal titanates is detected in a high concentrated alkali solution and the intensity of rutile phase decreases by the increase of hydrothermal time. Part of rutile phase is changed into sodium titanate as proved by UV-vis spectra within 24 h (Fig. 2e). All the rutile phase is disappeared after 10 days hydrothermal treatment at 130 °C evidenced by XRD. (Fig. S5). Fig. 2f shows the BET surface area change after experiencing the hydrothermal treatment. The BET surface areas of three titania samples P25, P25-700-1 and P25-800-8 steadily increase till the hydrothermal time of 12 h, and their BET surface areas at 12 h are 123, 186 and 74 m²/g, respectively. Further increase of the hydrothermal time to 24 h only gives a little higher surface areas.



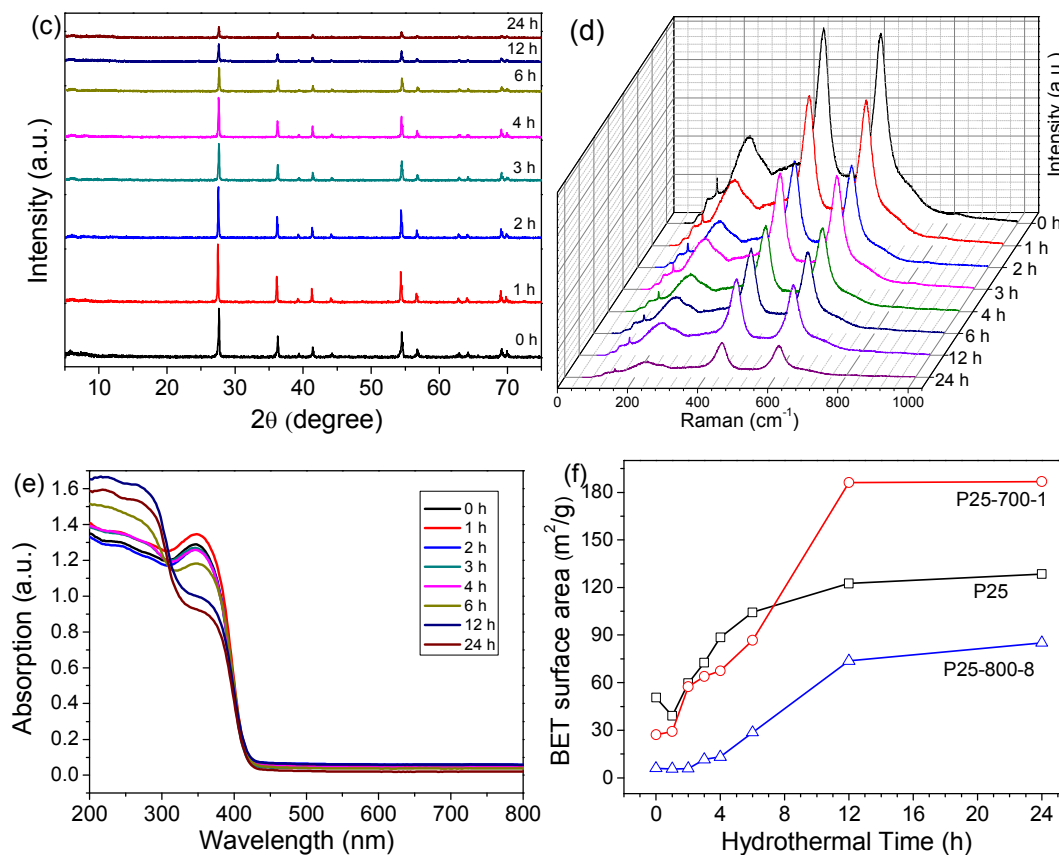


Fig. 2. XRD patterns (a, c) and Raman spectra (b, d) of hydrothermal treated products at 130 °C for 0-24 h using P25 (a, b) and P25-800-8 (c, d) as the starting material, UV-vis spectra (e) of hydrothermal treated P25-800-8 and BET surface areas (f) of the hydrothermal treated products.

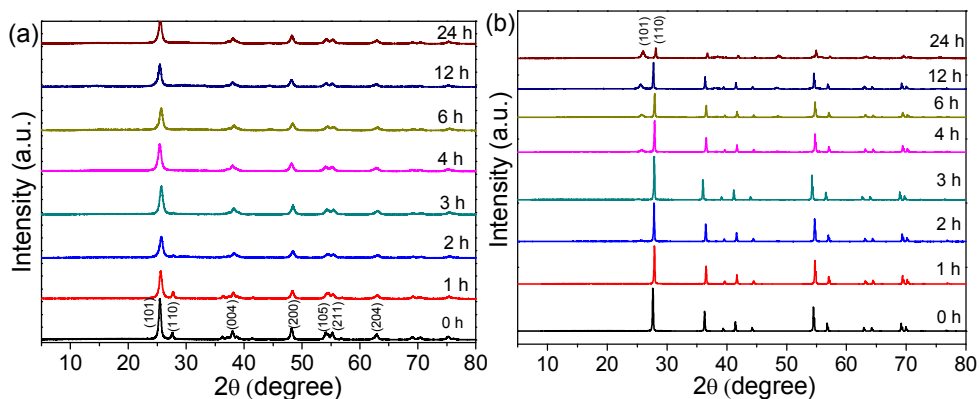


Fig. 3. XRD patterns of samples hydrothermally treated at 130 °C for 0-24 h and sintered at 400 °C for 5 h using P25 (a) and P25-800-8 (b).

The hydrothermal treated titania were calcined at 400 °C for 5 h and their XRD patterns are displayed in Fig. 3. By using P25 as the starting material, P25 changes into sodium titanate, then to hydrogen titanate after hydrothermal treatment and wash with deionized water. The calcination makes the products transform into pure anatase TiO₂ (Fig. 3a). However, by using pure rutile (P25-800-8) as the starting material, rutile

phase is much stable than anatase phase. Only part of rutile phase changes into sodium titanate/hydrogen titanate after hydrothermal treatment and wash with deionized water. The final products after calcination at 400 °C for 5 h have anatase and rutile phases (Fig. 3b) because that hydrogen titanate changes into anatase TiO₂.

3.3 Tubular structure formation

Fig. 4 shows TEM images of P25, P25-800-8 and the corresponding hydrothermal and post treated products. P25 is composed of nanosized particles with sizes of 30-40 nm (Fig. 4a). After hydrothermal and post treatment, the particles transform into short nanotubes with holes on the surface (Fig. 4b,c). For the pure rutile P25-800-8, the particle sizes increase to 150-300 nm (Fig. 4d), and the particles change into long nanotubes (Fig. 4e,f) by the same process. The resulting nanotubes have a very smooth surface and hardly any defects (Fig. 4f).

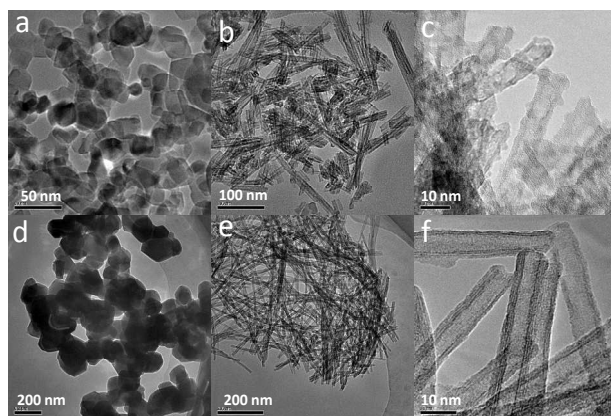


Fig. 4 TEM images of P25 (a) and P25-800-8 (d) and the hydrothermal products synthesized at 130 °C for 24 h in 10 M NaOH and calcined at 400 °C for 5 h by using P25 (b,c) and P25-800-8 (e,f).

3.4 The mechanism of phase transition of titania-based nanotube

Some valuable points can be obtained based on the above results: (1) Rutile phase is more stable than anatase in the hydrothermal process; (2) the mechanism of phase transition is different from that of morphological characteristics. By capturing the intermediate nanostructures at 130 °C, we proposed the process occurs in the hydrothermal treatment. During the hydrothermal process, the rutile nanoparticles (Fig. 5a) quickly coalesce (Fig. 5b), followed by exfoliation from large aggregated moieties in their peripheries into lamellars (Fig. 5c). The results agree well with our previous work,²³ where the evolution mechanism of titanate nanostructures in the hydrothermal process is systematically studied. The high-resolution TEM image of lamellars exfoliated from large aggregated moieties indicates that the dominated (110) facet of rutile were not observed (Fig. 5d and inset). The evidence clearly points out that the lamellar exfoliate from (110) facet. Then the lamellars rolls up to form short nanotubes. Afterwards, the short nanotubes transform into long ones through head-to-head attachment (OA mechanism) and OR ripening (Fig. 4e), evidenced by the semi-evolved nanostructure in Ref. 23. Here, the OA mechanism plays a vital role on morphological characteristics throughout the hydrothermal process.²³ However, the composition and crystal structure of nanotubes are not depended on the above

mechanism, and the dissolution-recrystallization mechanism plays a key role in the process. Rutile phase is more stable in the hydrothermal process. After the lamellar exfoliation from (110) facet, a little of rutile phase reacts with sodium hydroxide and generates sodium titanate, and then dissolves in the solution. Then sodium titanate recrystallizes on the surface of various nanostructures (such as lamellars and nanotubes). However, the amount of sodium titanate recrystallizing on the surface of various nanostructures is up to anatase phase ratio of raw materials (Fig. 2a). The amount of sodium titanate is so tiny that no characteristic peaks of sodium titanate are detected by XRD and Raman (Fig. 2c, d). Amorphous form of sodium titanate is only detected by UV-vis spectra (Fig. 2e). The so-called rutile TiO₂ nanotubes synthesized by a simple hydrothermal reaction under the assistance of ethanol at low-temperature is just because amorphous form of sodium titanate is not detected by XRD and Raman.²⁸ The amorphous form of sodium titanate can be proved after wash and calcinations (Fig. 3b). Pure anatase nanotubes using P25 as a raw material remain tubular structure, which possesses a lot of defects owing to a great quantity of dehydration (Fig. 5f). Obviously, the anatase nanotubes were short owing to breaking from the defects of them by calcination. And anatase and rutile nanotubes using P25-800-8 as a raw material have a perfect and long tubular structure (several nanometers to several micrometers in length) with a small amount of dehydration (Fig. 5e,g). The results clearly point out that pure titania nanotube with different phase ratios can be obtained using different kinds of titania as raw materials. Dissolution-recrystallization mechanism in hydrothermal process should affect the composition and crystal phase of products other than morphological characteristics.

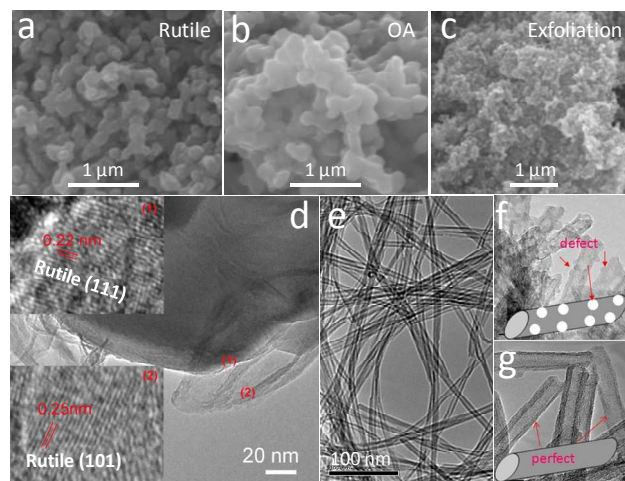


Fig. 5. The mechanism of phase transition of titania-based nanotubes via hydrothermal and post treatment. SEM images of pure rutile (P25-800-8, a) that experiences the oriented attachment (b) and exfoliation (c), TEM images of the exfoliated structure (d) and lattice spacings (inset), and the resulting nanotubes prepared pure rutile (e, g) and P25 (f).

4. Conclusions

Commercial TiO₂ P25 with anatase/rutile ratio of 80/20 changes into sodium titanate nanostructure after hydrothermal treatment at 150 °C for 120 h, and then to hydrogen titanate after washing. High temperature calcination at 400 °C for 5 h produces pure anatase nanotubes. At a lower hydrothermal temperature of 130 °C, TiO₂ P25 also transfers to sodium titanate, hydrogen titanate and anatase after hydrothermal treated over 2 h, washing with water and calcination at 400 °C for 5 h. The final tubular structure possesses a lot of defects owing to a great quantity of dehydration. However, pure rutile is more stable than titania P25. Only small amount of rutile transfers to amorphous sodium titanate after hydrothermal treatment at 130 °C within 24 h. Lamellars exfoliated from (110) facets of aggregated rutile particles roll up into nanotubes. The small amount of amorphous sodium titanate recrystallizes on the surface of nanotubes and produces a perfect tubular structure with only a small amount of dehydration after washing and calcination. Therefore, dissolution-recrystallization mechanism in hydrothermal process is an important step in the composition and crystal structure of titania-based nanotubes.

Acknowledgements

This research was financially supported by National Natural Science Foundation of China (Project U1332107) and Scientific and Technological Innovation Programs of Higher Education Institutions in Shanxi (2013137). J.Y. thanks the financial support from Natural Science Key Project of the Jiangsu Higher Education Institutions (15KJA220001), Jiangsu Specially-Appointed Professor Program and the Priority Academic Program Development of Jiangsu Higher Education.

Notes and references

1. M. Hernández-Alonso, S. García-Rodríguez, B. Sánchez and J. Coronado, *Nanoscale*, 2011, 3, 2233-2240.
2. T. Kasuga, M. Hiramatsu, A. Hoson, T. Sekino and K. Niihara, *Langmuir*, 1998, 14, 3160-3163.
3. T. Kasuga, M. Hiramatsu, A. Hoson, T. Sekino and K. Niihara, *Adv. Mater.*, 1999, 11, 1307-1311.
4. C.-C. Tsai and H. Teng, *Chem. Mater.*, 2004, 16, 4352-4358.
5. Y. V. Kolen'ko, K. A. Kovnir, A. I. Gavrillov, A. V. Garshev, J. Frantti, O. I. Lebedev, B. R. Churagulov, G. Van Tendeloo and M. Yoshimura, *J. Phys. Chem. B*, 2006, 110, 4030-4038.
6. R. Menzel, A. M. Peiró, J. R. Durrant and M. S. Shaffer, *Chem. Mater.*, 2006, 18, 6059-6068.
7. N. Murakami, T.-a. Kamai, T. Tsubota and T. Ohno, *Crystengcomm*, 2010, 12, 532-537.
8. Y. Suzuki, S. Pavasupree, S. Yoshikawa and R. Kawahata, *J. Mater. Res.*, 2005, 20, 1063-1070.
9. Y. Lan, X. Gao, H. Zhu, Z. Zheng, T. Yan, F. Wu, S. P. Ringer and D. Song, *Adv. Funct. Mater.*, 2005, 15, 1310-1318.
10. A. Nakahira, W. Kato, M. Tamai, T. Isshiki, K. Nishio and H. Aritani, *J. Mater. Sci.*, 2004, 39, 4239-4245.
11. L. T. Mancic, B. A. Marinkovic, P. M. Jardim, O. B. Milosevic and F. Rizzo, *Cryst. Growth Des.*, 2009, 9, 2152-2158.
12. B. Vijayan, N. M. Dimitrijevic, T. Rajh and K. Gray, *J. Phys. Chem. C*, 2010, 114, 12994-13002.
13. J. Yu, H. Yu, B. Cheng and C. Trapalis, *Journal of Molecular Catalysis A: Chemical*, 2006, 249, 135-142.
14. E. Morgado, M. A. de Abreu, G. T. Moure, B. A. Marinkovic, P. M. Jardim and A. S. Araujo, *Chem. Mater.*, 2007, 19, 665-676.
15. J. Huang, Y. Cao, Q. Huang, H. He, Y. Liu, W. Guo and M. Hong, *Cryst. Growth Des.*, 2009, 9, 3632-3637.
16. Á. Kukovecz, M. Hodos, E. Horváth, G. Radnóci, Z. Kónya and I. Kiricsi, *J. Phys. Chem. B*, 2005, 109, 17781-17783.
17. E. Horváth, Á. Kukovecz, Z. Kónya and I. Kiricsi, *Chem. Mater.*, 2007, 19, 927-931.
18. A. Elsanousi, E. Elssfah, J. Zhang, J. Lin, H. Song and C. Tang, *J. Phys. Chem. C*, 2007, 111, 14353-14357.
19. B. Yao, Y. Chan, X. Zhang, W. Zhang, Z. Yang and N. Wang, *Applied Physics Letters*, 2003, 82, 281-283.
20. X. Wu, Q.-Z. Jiang, Z.-F. Ma and W.-F. Shangguan, *Solid State Commun.*, 2007, 143, 343-347.
21. C.-C. Tsai and H. Teng, *Chem. Mater.*, 2006, 18, 367-373.
22. Q. Chen, W. Zhou, G. Du and L.-M. Peng, *Adv. Mater.*, 2002, 14, 1208-1211.
23. H. Q. Lu, J. H. Zhao, L. Li, J. F. Zheng, L. X. Zhang, L. M. Gong, Z. J. Wang and Z. P. Zhu, *Chem. Phys. Lett.*, 2011, 508, 258-264.
24. Z. Y. Yuan and B. L. Su, *Colloid. Surf. A*, 2004, 241, 173-183.
25. E. Horvath, A. Kukovecz, Z. Konya and I. Kiricsi, *Chem. Mater.*, 2007, 19, 927-931.
26. D. Wu, J. Liu, X. N. Zhao, A. D. Li, Y. F. Chen and N. B. Ming, *Chem. Mater.*, 2006, 18, 547-553.
27. R. Ma, K. Fukuda, T. Sasaki, M. Osada and Y. Bando, *J. Phys. Chem. B*, 2005, 109, 6210-6214.
28. J. Yan, S. Feng, H. Lu, J. Wang, J. Zheng, J. Zhao, L. Li and Z. Zhu, *Mater. Sci. Eng. B*, 2010, 172, 114-120.